eprints@whiterose.ac.uk
https://eprints.whiterose.ac.uk/

FABRICS-SHEAR STRENGTH LINKS OF SILICON-BASED

GRANULAR ASSEMBLIES

S. Judes Sujatha

Department of Civil Engineering
University College of Engineering
Nagercoil, India

Z. K. Jahanger

Department of Water Resources Engineering
College of Engineering
University of Baghdad
Baghdad, Iraq

S. Barbhuiya

School of Civil Engineering
University of Leeds
Leeds LS2 9JT, UK

S. Joseph Antony*

School of Chemical and Process Engineering
University of Leeds
Leeds LS2 9JT, UK

ABSTRACT

Silicon (Si)-based materials are sought in different engineering applications including Civil, Mechanical, Chemical, Materials, Energy and Minerals engineering. Silicon and Silicon dioxide are processed extensively in the industries in granular form, for example to develop durable concrete, shock and fracture resistant materials, biological, optical, mechanical and electronic devices which offer significant advantages over existing technologies. Here we focus on the constitutive behaviour of Si-based granular materials under mechanical shearing. In the recent times, it is widely recognised in the literature that the microscopic origin of shear strength in granular assemblies are associated with their ability to establish anisotropic networks (fabrics) comprising strong-force transmitting inter-particle contacts under shear loading. Strong contacts pertain to the relatively small number of contacts carrying greater than the average normal contact force. However, information on how such fabrics evolve in Si-based assemblies under mechanical loading, and their link to bulk shear strength of such

---

* Corresponding author (S.J.Antony@leeds.ac.uk)

assemblies are scarce in the literature. Using discrete element method (DEM), here we present results on how Si-based granular assemblies develop shear strength and their internal fabric structures under bi-axial quasi-static compression loading. Based on the analysis, a simple constitutive relation is presented for the bulk shear strength of the Si-based assemblies relating with their internal fabric anisotropy of the heavily loaded contacts. These findings could help to develop structure-processing property relations of Si-based materials in future, which originate at the microscale.

Keywords: Si, SiO$_2$, granular materials, micromechanics, shear strength, DEM.

1. INTRODUCTION

Micro fabrics of granular materials and their links to structure-property-processing relations under external loading environments are important to understand in different engineering applications [1-3]. Materials composed of particles and grains at small scales have many exciting properties that are very different from the same material composed of large particles. In particular, Silicon-based granular materials are used in many engineering applications. They are manufactured through several process treatments, for example, using mechanical [4], thermal [5, 6], electrical [5] and chemical treatments [5,7,8]. Their mechanical properties at small scales could differ from that of macro scale. For example, material bulk parameter such as Young's modulus differs by several orders of magnitude than those parameters determined theoretically by extrapolating from the atomic bond strengths up to the macroscopic scale [9]. Furthermore, different manufacturing routes of the particles [10] could result variations in their grain-scale properties, which in turn could alter their functional properties [11, 12, 13]. Particle-scale properties such as friction coefficient of granular materials could influence on the product quality in the additive manufacturing of structures [14]. However, detailed information is still scarce in the literature on how internal fabric measures link to the bulk strength characteristics, and the effects of particles scale properties on them for key materials such as Silicon (Si) and Silicon dioxide (SiO$_2$) in granular form.   In the current research, progresses are reported on the influence of single-particle scale properties on the evolution of different measures of the internal fabrics for different cases of Si (with variations in inter-particle friction) and SiO$_2$ granular assemblies subjected to bi-axial compression, and their link to bulk shear strength characteristics using computer simulations.

2. MATERIALS AND METHODS

 The simulations were carried out using Discrete Element Method (DEM), which was originally developed by Cundall and Strack [15] for studying the mechanical behaviour of assemblies of circular disk (2D) and sphere

(3D) shape granular assemblies. OVAL DEM software has been used in this study to simulate the micromechanical behaviour of granular assemblies [16]. The advantage of using DEM to simulate the mechanical behaviour of granular materials is its ability to give more information about what happens inside the assemblies at grain-scale under mechanical loading.   The method models the interaction between contiguous particles as a dynamic process and the time evolution of the particles is advanced using an explicit finite difference scheme [15]. A linear spring-dashpot contact force mechanism, as outlined by Cundall and Strack [15], was employed between contacting particles. Linear normal and tangential contact springs were assigned with equal values of stiffness. Previous studies (though for non-Si based granular assemblies) indicate that stiffness ratio seems to have relatively more influence on the force-fabrics in the non-spherical (/equivalent non-circular in 2D) particulate assemblies, than on the fabrics of round-shaped particulate assemblies [17]. However it would be interesting to examine the potential variations in the stiffness ratio of Si-based particles in future. Slipping between particles would occur whenever the contact friction attains the specified coefficient of inter-particle friction in the different samples C1-C4 (Table 1) considered in this study [18-22]. The Si samples C1-C3 accounted for the variations in the values of the inter-particle friction with the sample C3 having its maximum value. The properties of the sample C4 corresponds to a typical case of SiO_2. The Si-based granular assemblies studied here had identical initial packing fraction, and the individual shape of the particles (/grains) was circular.   The assemblies each contained 4096 particles with dense packing (initial solid fraction and coordination number which refers to the average number of contacts per particle were 0.848 and 3.8 respectively). All the granular assemblies studied here were poly-dispersed with the particle sizes ranged between 0.4 and 1.3 times the mean size 100 μm. The particle assemblies were initially random, isotropic and homogeneous and the initial indentations were less than 0.02% of D_{50}.

Table1 Properties of the grains used in the four granular assemblies.

Samples (C1-C4)	Density (kg/m³)	Spring constant K (N/m)	Coefficient of inter-particle friction
C1: Si	2330	0.3	0.16
C2: Si	2330	0.3	0.30
C3: Si	2330	0.3	0.38

C4: SiO$_2$	2200	0.3	0.30

The assemblies were compacted from an initial sparse state by artificially removing friction between particles and then isotropically reducing the area until the desired packing fraction was attained. The friction was then gradually introduced in small increments of time-step to the required value in the simulations. At the end of isotropic compression, the microstructure of the samples was confirmed as isotropic i.e. the orientation of the contacts did not present any bias along the principal directions [23]. The fabrics of the contacts are defined later. The assemblies were tested in a periodic cell. During the bi-axial compression simulations (two dimensional tests), the height of the assembly was reduced at a constant rate (along x_2 direction), while maintaining constant horizontal stress σ_{11} (Figure 1). The vertical strain was advanced in small increments of $\Delta \varepsilon_{22} = 1.0 \times 10^{-6}$, and several relaxation steps were performed within each increment. These measures minimized the transient inertial effects that would have otherwise biased the results of a presumed quasi-static loading.
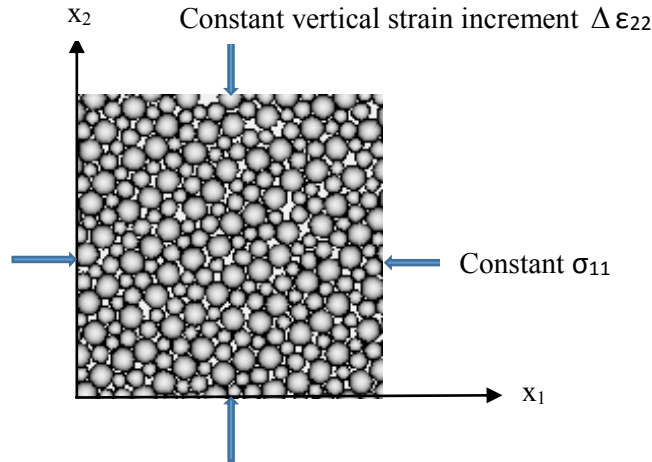

Fig. 1: Schematic diagram of the granular sample subjected to shearing

The fabrics of the contact orientation can be characterised using the definition suggested by Satake [24] as follows in Eq. (1):

$$\phi_{ij} = <n_i n_j> = \frac{1}{M} \sum_{1}^{M} n_i n_j$$

(1)

where, M is the number of contacts in the representative volume element and ni is the components of the unit normal vector at a contact between two contiguous particles. The deviator component of fabric tensor ϕ_{ij} is represented as follows in Eq. (2):

$$F = \phi_{22} - \phi_{11} \tag{2}$$

in which, ϕ_{22} and ϕ_{11} correspond to the value of ϕ along the major and minor principal directions respectively.

3. RESULTS AND DISCUSSION

We present the results for the micro-macroscopic shear deformation characteristics of the Si-based granular assemblies considered here with the focus on analysing the early stage (under small strains) mechanical response. The variation of macroscopic shear strength of the assemblies is presented in Figure 2 in a non-dimensional form. The macroscopic shear strength is presented in terms of the stress ratio q/p (q= $\sigma_{22}-\sigma_{11}$, p= $(\sigma_{22}+\sigma_{11})/2$, σ_{22} and σ_{11} are the major and minor principal stresses respectively) during the bi-axial compression of the assemblies. We observe that the variation of shear stress ratio q/p for the Si and SiO$_2$ particles are significantly different during early stages of compression, increasing with the inter-particle friction. This variation among the C3 case of Si and SiO$_2$ samples (Table 1) are fairly identical at small strains. Hence the relatively low value of the density of SiO$_2$ grains (but with the identical value of inter-particle friction as in the C3 case of the Si particles) has not affected their macroscopic shear strength. Detailed examinations are conducted below on how internal geometry measures and the fabric alignment of the grains in the assemblies evolve under the mechanical loading, and their potential links to the macroscopic shear strength.
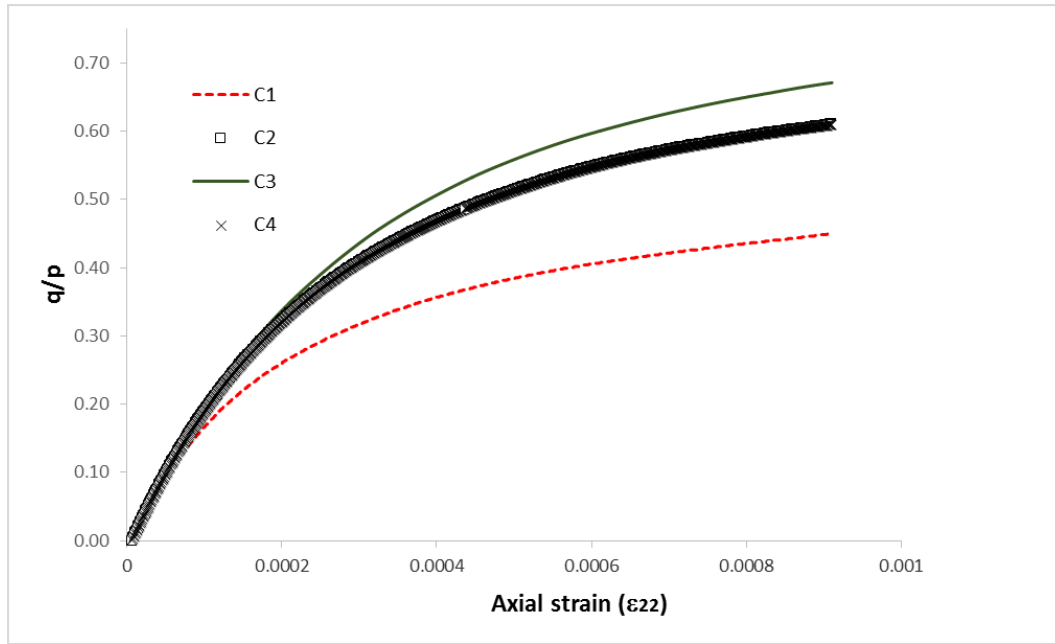
Fig. 2 Variation of the macroscopic shear stress ratio q/p of the assemblies.

The evolution of the number of contacts in the assemblies during bi-axial compression is presented in Figure 3. Interestingly, the Si-based assemblies experience an initial increase in the number of contacts, followed by a gradual reduction under further mechanical loading. The C1 case sample presents the highest value in the number of contacts at all stages of shearing, which could be associated with its particles having the lowest value of inter-particle friction [22]. The comparison of Figure 3 with Figure 2 suggests that no direct correlations exist between the shear strength and total number of contacts in the Si-based assemblies under mechanical loading. Indeed, the Si assembly (Case C3) with the highest magnitude of the shear stress ratio had the lowest number of contacts almost under all stages of loading, thus indicating a possible non-homogeneous and complex load sharing fabrics prevailing during shearing [25].

Recent studies show that, granular assemblies subjected to even uniform boundary loading could result non-homogeneous distribution of contact forces. The nature of the force distribution in the contacts of the particles depends on the individual properties of the particles and the packing arrangements [25-29]. Inspired by these results, we analysed for the directional orientations (fabrics) of the force transmission contacts in the Si-based assemblies under mechanical loading.
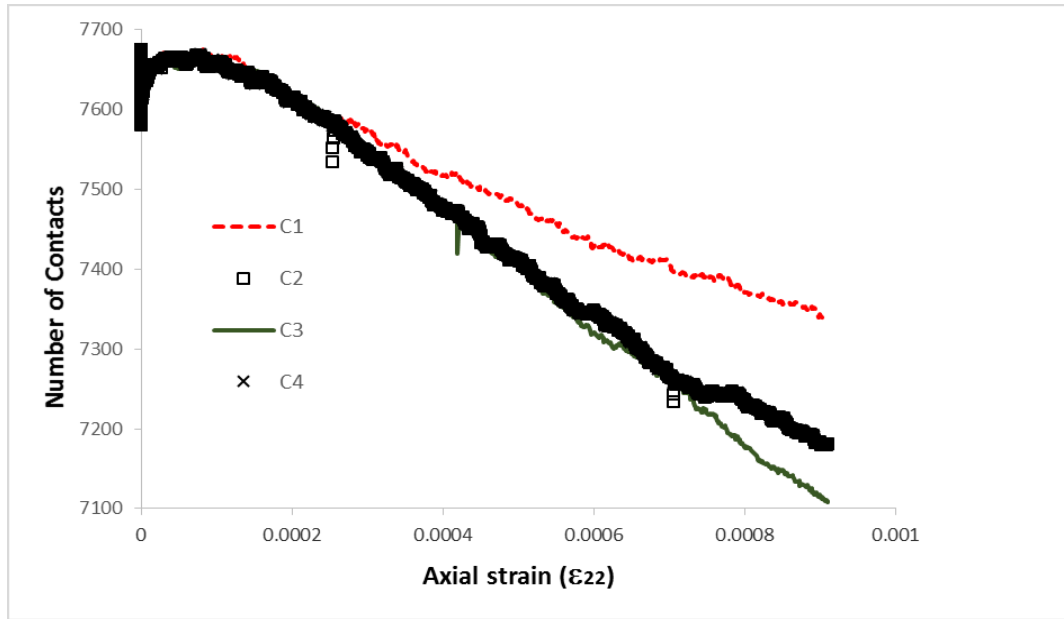
Fig. 3 Dynamic variation of the number of contacts in the assemblies.

Figure 4 shows the proportion of the contacts carrying greater than the average normal contact force at a given stage of loading in the assemblies, which are referred to as strong contacts (/heavily loaded contacts). It is evident that, in general, the Si system with the lowest value of inter-particle friction (Case C1) exhibits the lowest proportion of strong contacts and vice versa for the sample with the highest value of inter-particle friction (Case C3) under external loading.

Figure 5 shows a typical plot of force networks observed in the Si (Case C3) assembly at the steady stage of the compression loading. The black lines in this plot represent the normal contact force distribution and the thickness of the lines (branch vectors [15]) is proportional to the magnitude of the normal contact force. While the nature of force distribution network is seen as entirely non-homogeneous, it is observed that the strong force networks (represented by thick lines) generally aligned along the major principal stress direction (vertical direction in Figure 4). In Figure 5, the sliding contacts (red and blue lines) are also superimposed. This helps us to identify the contacts at which frictional sliding is dominant. The thickness of the branch vector is proportional to the rate of frictional sliding.
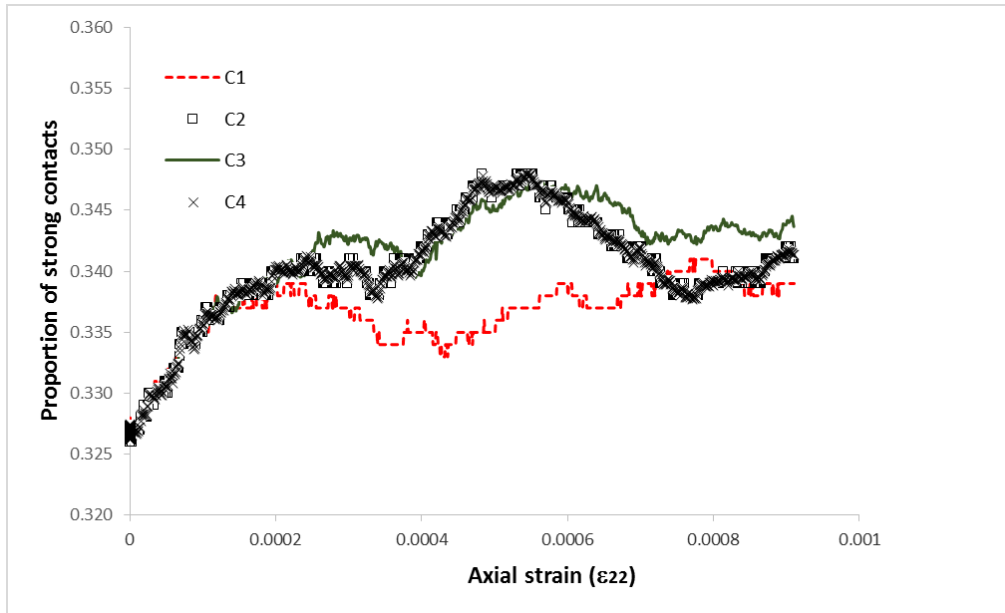
Fig. 4 Variation of the proportion of strong contacts in the assemblies under external loading.
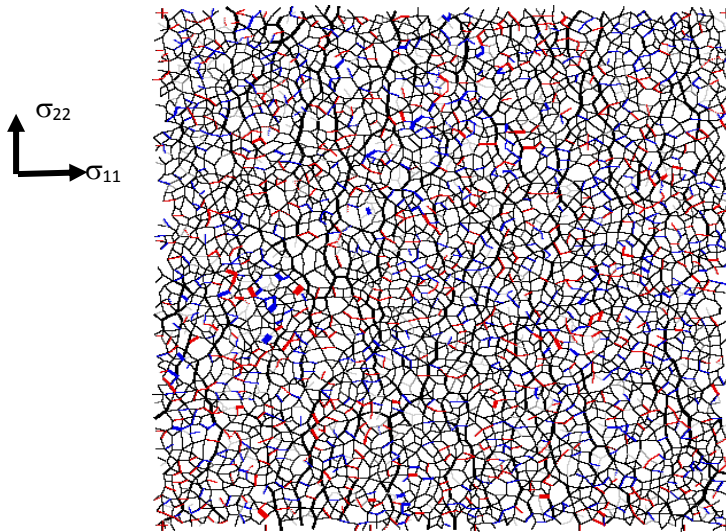

Fig. 5 Force networks and sliding contacts in the typical Si assembly (Case C3) under the steady stage of loading.

The red lines correspond to positive sliding (clockwise) while the blue lines represent the negative (anticlockwise) sliding. Generally, the sliding of the contacts occurs predominantly in the relatively week contacts entangled by the strong force transmitting contacts [23].

Figure 6 presents the comparison of the number of sliding contacts for the typical cases of Si (Case C3) and SiO$_2$ granular assemblies at the steady stage of compression. The relatively high level of sliding of contacts presented by the SiO$_2$ granular assembly could be attributed to the relatively low value of its inter-particle friction when compared with the Si (Case C3) assembly.
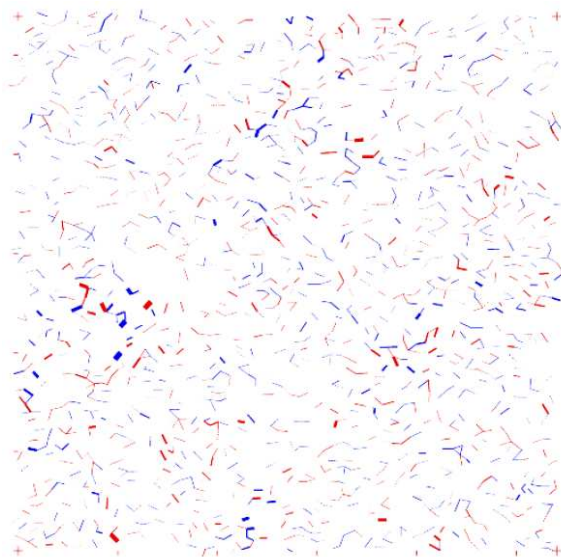
(a) Si assembly (Case C3)
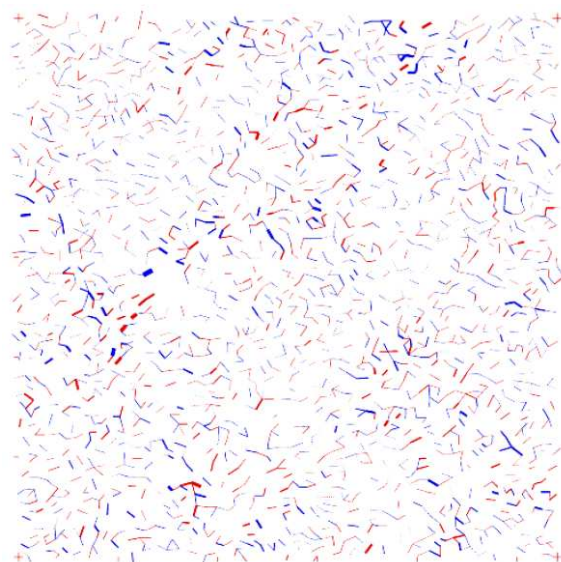
(b) SiO$_2$ assembly

Fig. 6 Comparison of sliding contacts between the Si (Case C3) and SiO$_2$ assemblies under steady stage of loading.

Next, detailed examinations are reported on the characteristics of the fabric alignment of the contacts in the assemblies during mechanical loading, with focus on examining their link to the macroscopic shear strength of the Si-based assemblies studied here. For this, the evolution of the topological measures faces, edges and vertices of the internal domains of the particles [2]. This is illustrated schematically in Figure 7, which shows the planar particle-connectivity graph (branch vectors) as suggested by Satake [24]. This could help to study the localised deformations within an area of interest. The connectivity graph can be modified further [2] by ignoring those particles having just one contact and no contacts, thus ignoring contacts that do not participate in distributing contact forces.
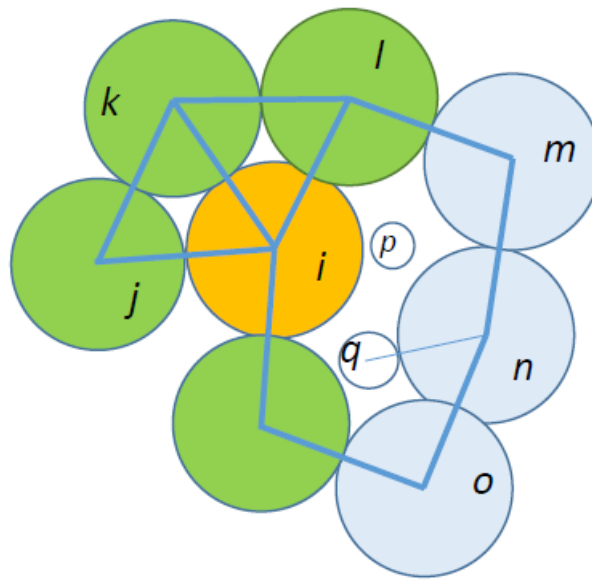

Fig. 7 Schematic representation of the particle connectivity graph of particles i, j…q. In this, the particle q has one contact and p has no contacts, while other particles have more than one contacts under a given stage of loading.

In this study, we generated this modified particle-connectivity graph and analysed their features, viz., and the evolution of number of faces (void cells), edges (contacts) and vertices (particles) [2] of the samples under the external loading and presented in Figs. 8-10. Previous studies on the mechanics of granular media have emphasised the usefulness of studying these measures [2]. For example, slipping and energy dissipation are associated to occurring at particle contacts which form the edges, and deformation occurs within the void cells that form the faces of the particle-connectivity graph [2]. In Figs. 8-10, these measures generally tend to be

high for the Case C1 of the Si assembly and relatively low in the Case C3 of the Si assembly. As we could expect, these results correspond to the frictional effects of the particles, with Case C1 having the relatively low value (0.16) and Case C3 with the high value (0.38) of inter-particle friction of the particles in the granular assemblies studied here. However, these variations do not appear to have a strong correlation to the shear strength (q/p) of the Si-based granular assemblies. To examine this, investigations were focused on the variation of the fabric alignment of strong contacts in the granular assemblies as described below.

Fig. 8 Evolution of the faces in the assemblies under external loading.

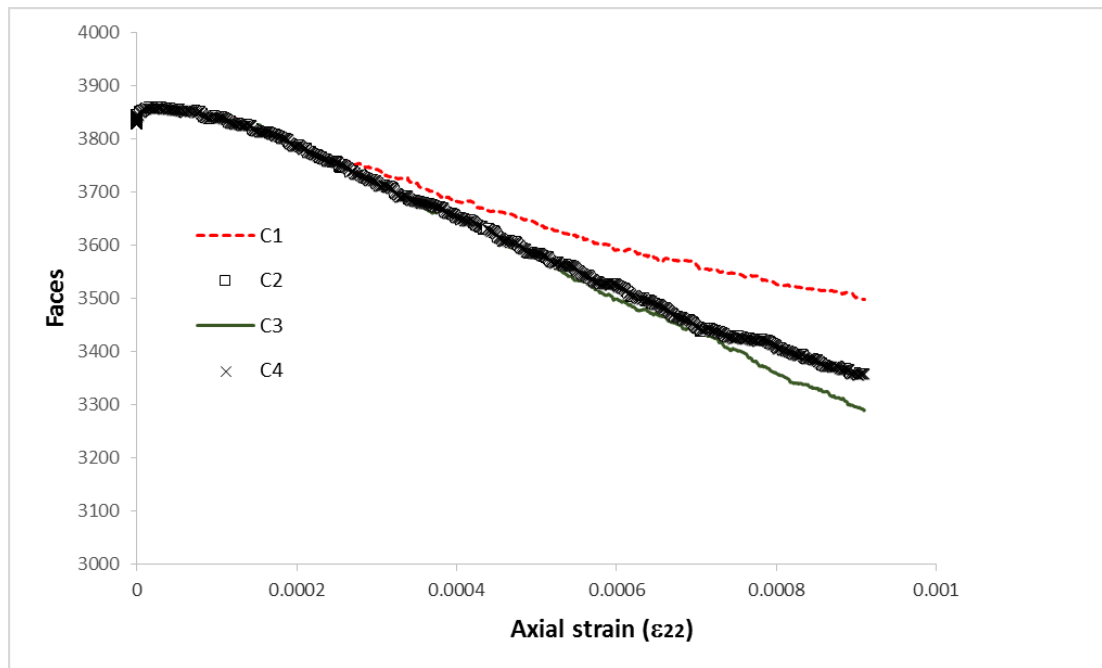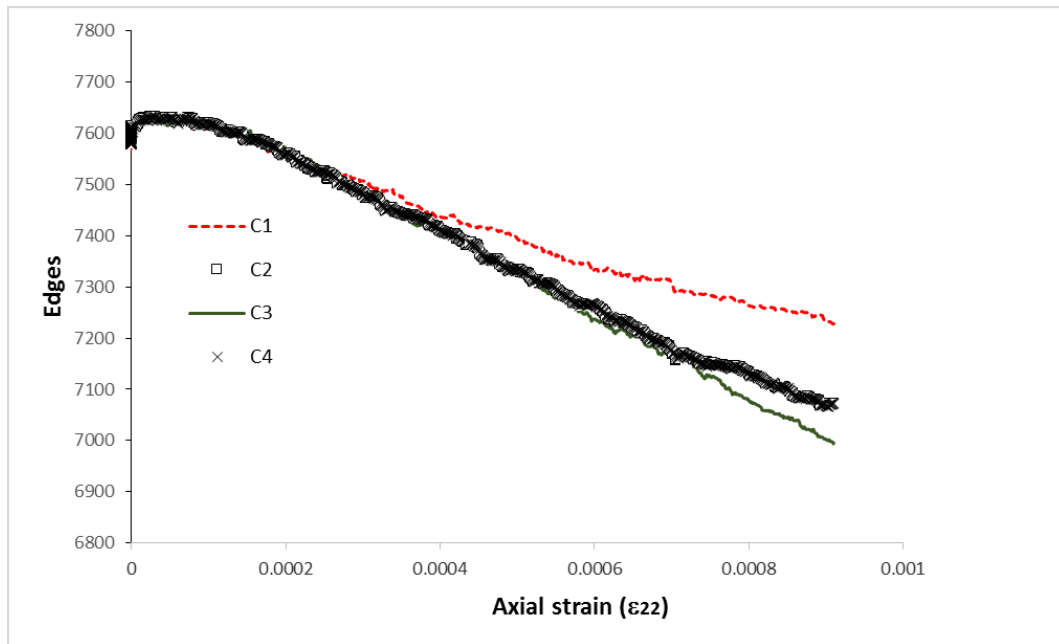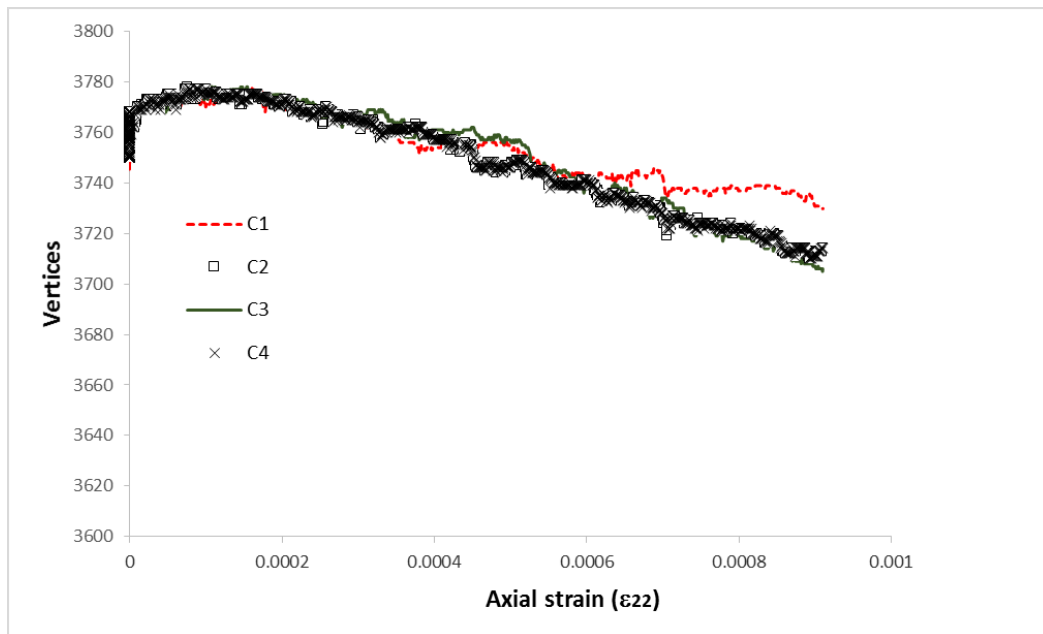Fig. 9   Evolution of the edges in the assemblies under external loading.

Fig. 10 Evolution of the vertices in the assemblies under external loading.

Though not presented here, a detailed analysis was conducted to identify correlation between the fabric anisotropy and shear stress ratio q/p, which turned out to be not strong. However, when the calculation of F

(Eq. (2)) accounted for the strong contacts only, referred to as Fs, the evolution of Fs agrees with q/p (both qualitatively and quantitatively) as presented in Figure 11 for all cases of Si-based granular assemblies studied here.
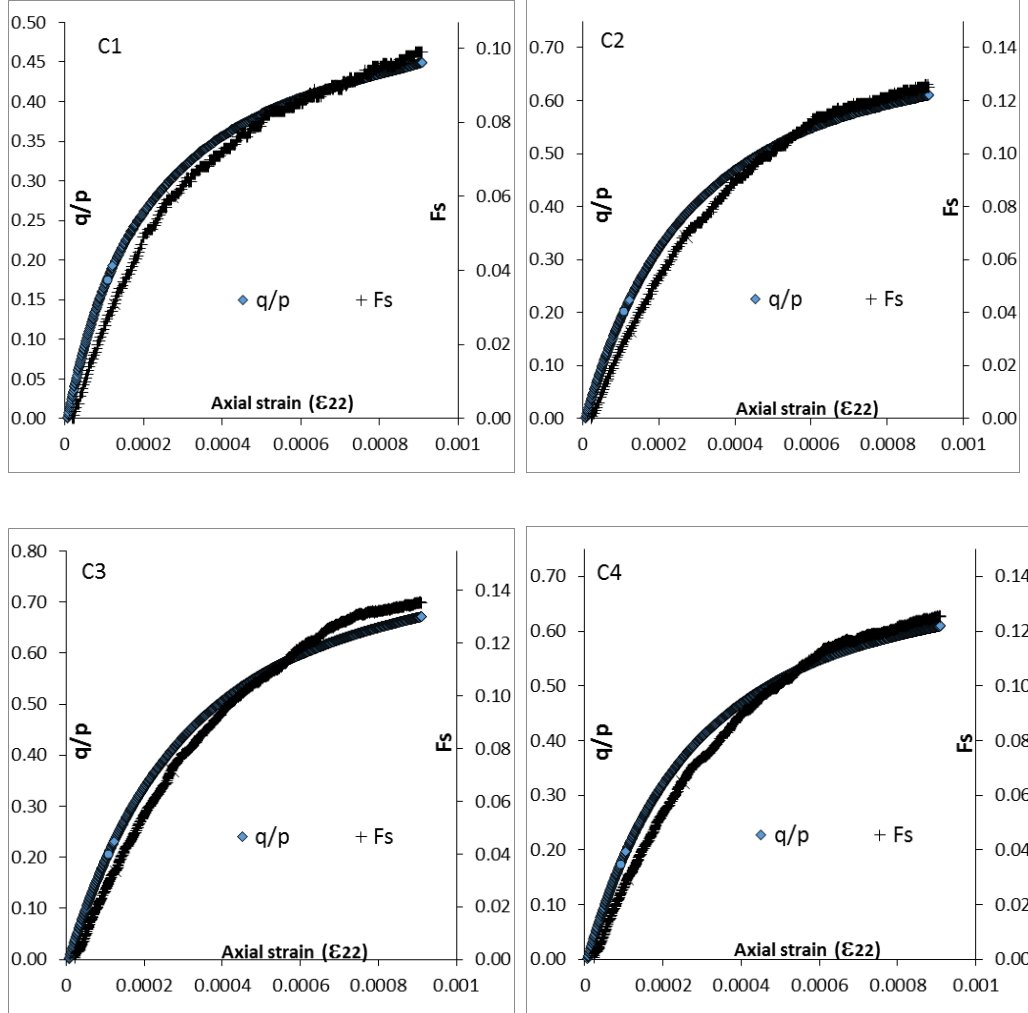
Fig. 11 Variation of the macroscopic shear stress ratio (q/p) and fabric anisotropy of strong contacts (Fs) the Si assemblies during compression.

From these results, the following simple constitutive relation between the macroscopic shear strength q/p and the fabric anisotropy of the strong contacts Fs of the Si-based granular assemblies is obtained as Eq. (3):

$$q/p = \alpha F_s \tag{3}$$

In this, α is the scaling parameter of the strong fabrics, which varies between 4.673-5.163. The values of α for the individual samples are provided in Table-2. The increase in the inter-particle friction has

contributed to an increase in the value of α. This trend supports further that, in the Si-based granular assemblies considered here, particle-scale friction contributes to establish strongly anisotropic network of heavily loaded contacts (strong contacts) under shearing. These results confirm that, the microscopic origin of the shear strength of Si-based granular assemblies is associated with their ability to develop fabric anisotropy of strong contacts (Fs) under shearing. The simple constitutive relation characterised above is quite interesting, considering the heterogeneous and complex nature of granular assemblies under mechanical loading.

Table 2 Value of α for the granular assemblies

Samples (C1-C4)	α
C1: Si	4.673
C2: Si	5.000
C3: Si	5.163
C4: SiO_2	5.000

4. CONCLUSIONS

The micromechanical deformation characteristics of some of the commercially important Si-based granular media are presented in this study. The numerical methodology employed here allows us to visualise the deformation and strength characteristics at both micro and macro scales. It is evident that inter-particle friction contributes significantly to enhance the fabric anisotropy of the strong contacts, and thereby mobilises shear strength in the Si-based granular systems. The simple relation presented in Eq. (3) characterises the link between the complex internal load-transfer characteristics of Si-based granular assemblies and their bulk shear strength.

In general, the complex micromechanical behaviour of granular assemblies, including their force transmission features could be influenced by a range of particle-scale properties, geometric conditions and loading

conditions. Hence the research reported here for Si-based particles is to be expanded further in a number of ways. Further studies are required to elucidate the dimensionality effects on the micro-macroscopic deformation characteristics of the Si-based granular systems considered here. Furthermore, the current study has not considered the effects of possible cohesion and non-linearity in contact force-incremental displacement relations [30] between the individual Si-based particles on the formation of contact fabrics in the granular assemblies under external loading. More realistic contact force identification strategies are also desired in the DEM simulations [31]. It is also required to elucidate the effects of particle shape and their packing structures on the nature of force fabrics in Si-based granular assemblies under shearing. There is another level of packing effect to consider as well, i.e., variations in molecular level packing structures in different sizes of the Si-based particles, which could result different interface energy between them. Another aspect to consider is, plastic deformation in granular assemblies are mostly associated with either the inherent irreversible dislocation of the grains under external loading even if the grains are elastic, or when individual particles possesses plastic deformation characteristics. In the current study, the simulations considered the former case and the relation between internal force fabrics to bulk strength characteristics are likely to be preserved at higher shear strain levels than considered in the present study. However, future investigations are required to understand the above aspects in detail.

ACKNOWLEDGEMENT

REFERENCES

1. Kalidindi, S.R., "Microstructure Informatics," In: Rajan, K. (Eds.), *Informatics for materials science and engineering: data-driven discovery for accelerated experimentation and application*, Butterworth-Heinemann, pp.443-466 (2013).

2. Kuhn, M., "Structured deformation in granular materials," *Mechanics of Materials*, **31**(6), pp.407-429 (2003).

3. Oda, M., "Initial fabrics and their relations to mechanical properties of granular materials," *Soils and Foundations*, **12**, (1), pp.17-36 (1970).

4. Calka, A. and Wexler, D., "Mechanical milling assisted by electrical discharge," *Nature*, **419**, pp.147-151 (2002).

5. Mayo, M. J., Chen, D. J., Hague, D. C., Edelstein, A. S. and Cammarata, R. C., *Nanomaterials: Synthesis, properties and applications*, Institute of Physics Publications, Bristol, England, (1996).

6. Charit, I. and Mishra, R.S., "Ultrafine grained materials," *Proceeding of 3rd Ultrafine Grained Materials Symposium*, USA, (2004).

7. Cannas, C., Casu, M., Licheri, R., Musinu, A., Piccaluga, G., Speghini, A. and Bettinelli, M., "Eu3 -doped $Y2O3-SiO_2$ nanocomposite obtained by a sol-gel method," *Proceeding of MRS Online Proceedings Library Archive*, 676, (2001).

8. Safarian, J., Tranell, G. and Tangstad, M., "Processes for Upgrading Metallurgical Grade Silicon to Solar Grade Silicon," *Energy Procedia*, **20**, pp.88–97 (2012).

9. Qian, D., Wagner, G. J. and Liu, W. K., "Mechanics of carbon nanotubes," *Applied Mechanics Review*, **55**, (6), pp.495-533 (2002).

10. Schey, J.A., *Introduction to Manufacturing Processes*, McGraw Hill, NewYork, USA, (2000).

11. Koch, C.C., *Nano Structured Materials: Processing, Properties and Applications*, William Andrew, Norwich, USA, (2007).

12. Yu, T., Greish, K., McGill, L. D., Ray, A. and Ghandehari, H., "Influence of geometry, porosity and surface characteristics of Silica nanoparticles on acute toxicity: Their vasculature effect and tolerance threshold," *ACS Nano*, **6**, (3), pp.2289–2301(2012).

13. McDowell, D., Panchal, J., Choi, H., Seepersad, C., Allen, J. and Mistree, F., *Integrated Design of Multiscale, Multifunctional Materials and Products*, Butterworth-Heinemann, Amsterdam, Holland, (2010).

14. Rathee, S., Srivastava, M., Maheshwari, S., Kundra, T. K. and Siddiquee, A.N., *Friction Based Additive Manufacturing Technologies: Principles for Building in Solid State, Benefits, Limitations, and Applications*, CRC Press, London, England, (2018).

15. Cundall, P.A. and Strack, O.D.L., "A discrete numerical model for granular assemblies," *Geotechnique*, **29**, pp.47-65 (1979).

16. M.R. Kuhn, Granular Geomechanics, ISTE Press, London, 2017

17. Antony, S.J., Moreno-Atanasio, R., Hassanpour, A., "Influence of contact stiffnesses on the micromechanical characteristics of dense particulate systems subjected to shearing," *Applied Physics Letters*, **89**, 214103 (2006).

18. Materials database, http://www.memsnet.org/material/

19. Hansen, L.T., Kühle, A., Sørensen, A.H., Bohr J. and Lindelof, P.E., "A technique for positioning nanoparticles using an atomic force microscope," *Nanotchnology*, **9**, (4) pp.337-342 (1998).

20. Sun, L. and Gong, K., "Silicon-based materials from rice husks and their applications," *Industrial and Engineering Chemistry Research*, **40**, (25) pp.5861-5877 (2001).

21. Jung, M., Choi, S. S., Kang, C.J. and Kuk, Y., "Fabrication of bimetallic cantilevers and its characterisation," *Surface Review and Letters*, **6** (6), pp.1195-1199(1999).

22. Lynch, C. T., *Handbook of Materials Science Volume 1: General properties*, CRC Press, Cleveland, (1974).

23. Thornton, C. and Antony, S.J., "Quasi–static deformation of particulate media," *Philosophical Transactions of the Royal Society of London, Series:A*, **356** (1747), pp.2763-2782 (1998).

24. Satake M., "Fabric tensor in granular materials," In: Vermeer, P.A. and Luger, H.J. (Eds.), *Deformation and Failure of Granular Materials*, Balkema, Rotterdam, pp.63-68 (1982).

25. Antony, S.J. and Kruyt, N.P., "Role of interparticle friction and particle-scale elasticity on shear strength mechanism in three dimensional granular media," *Physical Review E*, **79**, pp.031308 (2009).

26. Antony, S.J., "Link between single-particle properties and macroscopic properties in particulate assemblies: role of structures within structures," *Philosophical Transactions of the Royal Society of London, Series:A*, **365**, pp.2879–2891(2007) .

27. Antony, S.J., "Evolution of force distribution in three-dimensional granular media," *Physical Review E, American Physical Society*, **63**(1), pp.011302 (2001).

28. Antony, S.J. and Ghadiri, M., "Size effects in slowly sheared granular media," *Journal of Applied*

Mechanics, American Society of Mechanical Engineers, **68** (5), pp.772-775 (2001).

29. O'Sullivan, C., *Particulate Discrete Element Modelling: A Geomechanics Perspective*, CRC Press, London, (2011).

30. Chung, Y.C., Wu, C.W., Kuo, C.Y., Hsiau, S.S., A rapid granular chute avalanche impinging on a small fixed obstacle: DEM modeling, experimental validation and exploration of granular stress. *Applied Mathematical Modelling*, **74**, 540-568, (2019).

31. D. Zhang, W.J. Whiten, The calculation of contact forces between particles using spring and damping models, Powder Technology, **88,** pp.59-64, (1996).

Figure captions

Fig. 1: Schematic diagram of the granular sample subjected to shearing

Fig. 2 Variation of the macroscopic shear stress ratio q/p of the assemblies.

Fig. 3 Dynamic variation of the number of contacts in the assemblies.

Fig. 4 Variation of the proportion of strong contacts in the assemblies under external loading.

Fig. 5 Force networks and sliding contacts in the typical Si assembly (Case C3) under the steady stage of loading.

Fig. 6 Comparison of sliding contacts between the Si (Case C3) and SiO_2 assemblies under steady stage of loading.

Fig. 7 Schematic representation of the particle connectivity graph of particles i, j…q. In this, the particle q has one contact and p has no contacts, while other particles have more than one contacts under a given stage of loading.

Fig. 8 Evolution of the faces in the assemblies under external loading.

Fig. 9 Evolution of the edges in the assemblies under external loading.

Fig. 10 Evolution of the vertices in the assemblies under external loading.

Fig. 11 Variation of the macroscopic shear stress ratio (q/p) and fabric anisotropy of strong contacts (Fs) the Si assemblies during compression.